B. R. Johnson

View Online **Export Citation**

ARTICLES YOU MAY BE INTERESTED IN

New numerical methods applied to solving the one-dimensional eigenvalue problem
The Journal of Chemical Physics **67**, 4086 (1977); https://doi.org/10.1063/1.435384

Matrix Numerov method for solving Schrödinger's equation
American Journal of Physics **80**, 1017 (2012); https://doi.org/10.1119/1.4748813

An improved log derivative method for inelastic scattering
The Journal of Chemical Physics **85**, 6425 (1986); https://doi.org/10.1063/1.451472
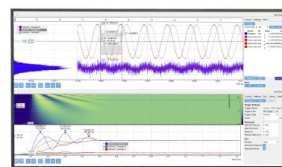
The renormalized Numerov method applied to calculating bound states of the coupled-channel Schroedinger equation[a]

B. R. Johnson

Chemistry and Physics Laboratory, The Ivan A. Getting Laboratories, The Aerospace Corporation, El Segundo, California 90245
(Received 16 June 1978)

The renormalized Numerov method, which was recently developed and applied to the one-dimensional bound state problem [B. R. Johnson, J. Chem. Phys. **67**, 4086 (1977)], has been generalized to compute bound states of the coupled-channel Schroedinger equation. Included in this presentation is a generalization of the concept of a wavefunction node and a method for detecting these nodes. By utilizing node count information it is possible to converge to any specific eigenvalue without the need of an initial close guess and also to calculate degenerate eigenvalues and determine their degree of degeneracy. A useful interpolation formula for calculating the eigenfunctions at nongrid points is also given. Results of example calculations are presented and discussed. One of the example problems is the single center expansion calculation of the $1s\sigma_g$ and $2s\sigma_g$ states of H_2^+.

I. INTRODUCTION

In a previous paper[1] we developed two new numerical procedures, the log derivative and renormalized Numerov methods, for calculating the bound state solutions of the one-dimensional Schrödinger equation. In this report the renormalized Numerov method (version B) which was the most efficient and easiest to program, is generalized to calculate bound state solutions of the coupled-channel Schrödinger equation. (The generalization of the log derivative method will also be discussed briefly in Appendix A.) This method has several noteworthy features. It is quite efficient of computer time. No initial guess close to the desired eigenvalue is required. Each solution is characterized by a unique "generalized node count," therefore, we can be sure we have not inadvertently skipped any solution. It can calculate degenerate eigenvalues and indicate their degree of degeneracy. The method is very stable, it converges to the solution specified by a given node count, even in cases of multiple classically allowed regions separated by classically forbidden regions. Finally, no overflow or linear dependence problems occur, so no special programing precautions have to be taken in this regard.

This paper is divided as follows. In Sec. II we formulate the problem and specify the conditions that the wavefunction must satisfy, a generalized node count is defined and the renormalized Numerov method for calculating eigenvalues is presented. Sec. III discusses the calculation of the eigenfunctions. Included is a generalization of the interpolation method derived in Ref. 1 for calculating the wavefunction at nongrid points. Finally, the results of several example calculations and a general discussion is presented in Sec. IV.

II. EIGENVALUE CALCULATIONS

A. Wavefunction methods

In many cases a multidimensional quantum mechanical problem can, to a good approximation, be transformed to a system of M coupled ordinary second order differ-

ential equations. Several examples of this will be given in Sec. IV. The resulting "coupled-channel Schrödinger equation" is most conveniently written in the following matrix differential equation form:

$$\left[\mathbf{I}\, \frac{d^2}{dx^2} + \mathbf{Q}(x) \right] \psi(x) = 0 \tag{1}$$

where

$$\mathbf{Q}(x) = (2\mu/\hbar^2)[E\mathbf{I} - \mathbf{V}(x)]. \tag{2}$$

Here, $\mathbf{I}$ is the unit matrix, μ is the reduced mass, $\mathbf{V}(x)$ is the symmetric potential matrix and E is the energy. The wavefunction $\psi(x)$ is a column matrix (or vector). Acceptable bound state wavefunctions must be continuous together with their first derivatives and must vanish at the boundaries

$$\psi(x) \xrightarrow[x \to \pm \infty]{} 0. \tag{3}$$

If x is a radial coordinate, the boundary condition at $-\infty$ is replaced by

$$\psi(0) = 0. \tag{4}$$

The wavefunctions (eigenfunctions) that satisfy these conditions can be calculated by an iterative procedure. A trial energy E is chosen along with trial values of the slopes of the wavefunction at the initial and final boundaries. Equation (1) is then integrated outward from the "inner" boundary and inward from the "outer" boundary to a common matching point. In general, the wavefunction and its first derivative calculated this way will not be continuous across the matching point and therefore not an eigenfunction. Fox[2,3] has devised an elaborate method for calculating new trial values of the energy and the initial derivatives at the boundaries which reduce the magnitude of the discontinuity. The calculation is iterated and eventually converges at a quadratic rate to an eigenvalue.

Gordon[4,5] has devised a much simpler method which entirely avoids the problem of searching for the correct values of the initial boundary derivatives. Instead of calculating a single solution vector using trial values for the derivatives, he calculates M linearly independent solutions with arbitrary (but linearly independent) derivatives and, of course, zero value at the bound-

aries. These M solution vectors can be grouped together to form the M columns of a single $M \times M$ square matrix wavefunction $\Psi(x)$ which satisfies the differential equation

$$\left[I \frac{d^2}{dx^2} + Q(x) \right] \Psi(x) = 0. \tag{5}$$

[This equation differs from Eq. (1) only in that the column vector $\psi(x)$ has been replaced by the square matrix $\Psi(x)$.] Since the columns of $\Psi(x)$ are linearly independent, they span the space of all possible initial derivatives. Therefore, the correct column vector wavefunction must be expressible as some (unknown) linear combination of the columns of $\Psi(x)$ i.e.,

$$\psi(x) = \Psi(x) \cdot C, \tag{6}$$

where C is a column vector of constant coefficients.

The Gordon procedure is to assume a trial value for the energy and then integrate Eq. (5) outward and inward to the common matching point x_m. The outward solution which approaches x_m from the left is designated $\Psi_l(x)$ and the inward solution which approaches from the right is $\Psi_r(x)$. If the trial energy is an eigenvalue, the eigenfunction vector is given by

$$\psi(x) = \Psi_l(x) \cdot l \quad x \le x_m \tag{7}$$

and

$$\psi(x) = \Psi_r(x) \cdot r \quad x \ge x_m, \tag{8}$$

where l and r are, as yet, unknown vectors. At the matching point the continuity of the eigenfunction and its first derivative require that

$$\Psi_l(x_m) \cdot l = \Psi_r(x_m) \cdot r = \psi(x_m) \tag{9}$$

and

$$\Psi_l'(x_m) \cdot l = \Psi_r'(x_m) \cdot r = \psi'(x_m). \tag{10}$$

These two matching conditions were combined by Gordon[4] in a super-matrix equation

$$\begin{pmatrix} \Psi_l(x_m) & \Psi_r(x_m) \\ \Psi_l'(x_m) & \Psi_r'(x_m) \end{pmatrix} \begin{pmatrix} l \\ -r \end{pmatrix} = 0. \tag{11}$$

The condition that Eq. (11) have a nontrivial solution is that the determinant of coefficients vanish, i.e.,

$$d(E) = \begin{vmatrix} \Psi_l(x_m) & \Psi_r(x_m) \\ \Psi_l'(x_m) & \Psi_r'(x_m) \end{vmatrix} = 0. \tag{12}$$

Thus, the determinant $d(E)$, which is a function of the trial energy E, will vanish at each of the eigenvalues. The search for the zeros of $d(E)$ can be carried out by any standard one-dimensional search method. Once an eigenvalue is located, the set of linear equations, Eq. (11), can be solved for the vectors l and r (to within an overall arbitrary normalization factor). These are then substituted in Eqs. (7) and (8) to obtain the eigenfunction vector. [The transformation of the Gordon procedure, described above, to the log derivative matrix formulation is discussed in Appendix A.]

The method described above has several limitations. We must start with an initial energy guess fairly near the eigenvalue that we wish to calculate, i.e., we can-

not converge to a specific eigenvalue (for example, the fourth eigenvalue above the ground state) from afar. Another problem is that we cannot be sure if we have skipped any of the eigenvalues. In the one-dimensional case both these limitations were overcome by counting nodes and applying the oscillation theorem[6] which states that if the eigenvalues are arranged in ascending order, then the eigenfunction $\psi_n(x)$ $(n = 0, 1, 2, \cdots)$ corresponding to the $(n+1)$th eigenvalue E_n has n nodes. In the multichannel case we can generalize the definition of a node so that the same methods can be applied.

The definition of "node" that we have found useful is that it is a zero of the determinant function $|\Psi(x)|$. In order to see why this is a useful definition imagine the following problem: At the left boundary place an infinite (inpenetrable) potential wall. This is consistent with the boundary condition that the wavefunction is zero at this point and does not affect the solution. As the integration of Eq. (5) proceeds from left to right imagine another infinite potential wall moving to the right with the integration. In the region between the walls the potential is just $V(x)$. Initially, all the eigenvalues of this imaginary problem are very large and positive, but as the walls move apart the eigenvalues monotonically decrease and approach the eigenvalues of the original problem as the right-hand wall approaches the final boundary. As the eigenvalues decrease, those that are eventually less than the trial energy E must at some point cross this energy. The position of the right-hand wall, when one of the eigenvalues of the imaginary problem just equals the trial energy E, is determined by the relation $|\Psi(x)| = 0$. This should be obvious, since this is the necessary and sufficient condition to calculate a wavefunction vector that is zero at this point and thus satisfy the coundary conditions at the right-hand wall. Thus, we conclude that the number of eigenvalues less than or equal to the trial energy E is just equal to the number of nodes of the function $|\Psi(x)|$.

Each discrete eigenvalue is labeled by assigning to it the integer n which is equal to the number of eigenvalues lying below it in value. This label is unique for the non-degenerate eigenvalues. Degenerate eigenvalues are assigned g consecutive integers from n through $n+g-1$ where g is the degree of degeneracy. It is obvious from our previous discussion that by counting the number of nodes of a trial solution we can determine if the trial energy E is above or below a specific eigenvalue E_n which has been labeled in this way. If the node count is greater than n, then $E \ge E_n$ and if the node count is less than or equal to n then $E < E_n$. These relations are the basis of a bisection procedure for calculating E_n. The initial step of this procedure is to calculate by some simple method crude upper and lower bounds, E_H and E_L, such that $E_L < E_n \le E_H$. Set the trial energy E equal to

$$E = 0.5(E_L + E_H), \tag{13}$$

then integrate Eq. (5) outward and count the number of nodes of $|\Psi(x)|$. If the node count is greater than n set $E_H = E$ and if it is less than or equal to n set $E_L = E$. Calculate a new trial energy using Eq. (13) and repeat the process. This method will converge linearly to the

desired eigenvalue. The iteration is stopped when $E_H - E_L < \epsilon$ where ϵ, the tolerance factor, is some preset small (positive) number. This procedure will work even if the eigenvalue is degenerate. The degree of degeneracy is given by the difference in node count for the final E_H and E_L values. [If two nondegenerate eigenvalues happen to be separated by less than the preset tolerance factor ϵ, this method will usually indicate that these eigenvalues are degenerate.]

Since linear convergence is rather slow, the best procedure is to combine the node count method, which can converge to a particular eigenvalue from afar, with a fast converging method such as the Gordon[4] procedure. The node count method is used to isolate a single eigenvalue and get sufficiently close to it, then the fast converging method takes over and very quickly converges to the desired accuracy. When an eigenvalue is one of a degenerate set of eigenvalues, it cannot be isolated. In such a case convergence will be entirely by the node count procedure.

In the one-dimensional problem, for a given energy E, the x coordinate can be divided into classically allowed and classically forbidden regions separated by classical turning points. The turning point with the smallest (or most negative) value is called the "inner turning point" and the one with the largest value is the "outer turning point." The region between the inner and outer turning points is called the "confinement region." The region to the left of (less than) the inner turning point is the "inner forbidden region" and the region to the right of (greater than) the outer turning point is the "outer forbidden region." Of course, the confinement region can be subdivided by classically forbidden subregions contained within it. For some problems, i.e., s-wave bound states in a purely attractive potential well, there is no inner forbidden region. For such a problem the confinement region is from $x = 0$ to the outer turning point.

This same discussion can be applied to the multichannel problem if the definitions are suitably generalized. These generalizations were established for the multichannel JWKB approximation.[7] Diagonalize the potential matrix $V(x)$ for all values of x. The result is the diagonal "adiabatic" potential matrix $U(x)$ with matrix elements $U_{ii}(x)$, $i = 1, M$. The M equations

$$U_{ii}(x_j) - E = 0 \quad (i = 1, M) \tag{14}$$

are solved for all the real roots x_j. The inner classical turning point is the smallest (or most negative) root and the outer classical turning point is the largest root. The definitions of the inner and outer classically forbidden regions and the confinement region are then the same as for the one-dimensional case.

The boundary conditions are given by Eqs. (3) and (4). In an actual calculation the integration range extends from an initial point x_i to a final point x_f and does not have to extend between the limits 0 to ∞ (or $-\infty$ to ∞). Rather, it is sufficient for x_i to be located in the inner forbidden region and x_f to be located in the outer forbidden region and far enough from the respective turning points so that the calculated eigenvalues are insensi-

tive to the values of the wavefunction at x_i and x_f. If there is no inner forbidden region, we must set $x_i = 0$. Convenient boundary values to use (which are also appropriate in the case where $x_i = 0$) are $\Psi(x_i) = \Psi(x_f) = 0$ and $\Psi'(x_i) = \Psi'(x_f) = \alpha I$ where α is an arbitrary number.

The methods discussed in this subsection could be implemented by solving Eq. (5) numerically for $\Psi(x)$. However, without taking special precautions, this procedure would have severe overflow and linear dependence problems. These difficulties do not occur with the renormalized Numerov method which is discussed next.

B. Renormalized Numerov method

The matrix Numerov algorithm is an efficient method that can be used to obtain numerical solutions of Eq. (5). The basic formula is the three term recurrence relation

$$[I - T_{n+1}]\Psi_{n+1} - [2I + 10T_n]\Psi_n + [I - T_{n-1}]\Psi_{n-1} = 0 \tag{15}$$

where

$$\Psi_n \equiv \Psi(x_n) \tag{16}$$

and

$$T_n = -(h^2/12)Q(x_n) \tag{17}$$

Here h is the spacing between the $N+1$ equally spaced grid points x_0, x_1, $\cdots x_N$ and the square matrix $Q(x)$ is defined by Eq. (2). Equation (15) is derived by an obvious generalization of the derivation of the ordinary Numerov algorithm[8] to matrix quantities.

The renormalized Numerov algorithm is derived from Eq. (15) by making two transformations. First, define the matrix

$$F_n = [I - T_n]\Psi_n \tag{18}$$

and substitute into Eq. (15). This gives

$$F_{n+1} - U_n F_n + F_{n-1} = 0, \tag{19}$$

where

$$U_n = (I - T_n)^{-1}(2I + 10T_n). \tag{20}$$

Next, define the ratio matrix

$$R_n = F_{n+1} F_n^{-1}. \tag{21}$$

Substitute this into Eq. (19) to obtain the two term recurrence relation

$$R_n = U_n - R_{n-1}^{-1}. \tag{22}$$

This is the basic equation of the renormalized Numerov method. It can be solved once the value of the initial term R_0 is specified. The initial grid point is located at $x_0 = x_i$ and the initial values of the wavefunction are $\Psi(x_0) = 0$ and $\Psi(x_1) \neq 0$. (See the discussion of boundary values in the previous section.) The corresponding value of the inverse of the initial term is $R_0^{-1} = 0$. (For exceptions to this rule see Appendix D.)

The matrix U_n, defined by Eq. (20), is symmetric. It follows from this and the symmetry of R_0^{-1} and also from Eq. (22) that the matrix R_n is also symmetric. For computational convenience, Eq. (20) can be reformulated as a symmetric matrix inversion problem. Define

$$W_n = I - T_n, \tag{23}$$

then

$$U_n = 12W_n^{-1} - 10I. \tag{24}$$

Thus, at each grid point we must invert two symmetric matrices.[9]

In the previous section we described a bisection method of calculating eigenvalues which was based on counting the nodes of the function $|\Psi(x)|$. This method is easily implemented in the renormalized Numerov formalism. In the present discussion we assume only a single node between two adjacent grid points. The case of multiple nodes will be discussed in Appendix B. It follows from Eqs. (18) and (21) (and also from the requirement[10] that $|I - T_n| > 0$) that $|R_n| < 0$ only if $|\Psi(x)|$ changes sign between x_n and x_{n+1}. Since $|\Psi(x)|$ is a continuous function it must have a node in this interval. It follows that we can count the nodes of $|\Psi(x)|$ by monitoring $|R_n|$ and counting the number of times it is negative. The calculation of the determinant $|R_n|$ at each step adds only insignificantly to the computation time since it can be carried out simultaneously with the calculation of the inverse matrix R_n^{-1}.

A fast converging method based on matching inward and outward solutions can also be derived. It is the multichannel generalization of the renormalized Numerov method B used in the one-dimensional problem.[1] This method is used for the final stages of convergence after we have isolated a particular eigenvalue by the node count procedure.

The inward solution is most conveniently expressed in terms of the matrix

$$\hat{R}_n = F_{n-1}F_n^{-1}. \tag{25}$$

Substituting this into Eq. (19), we obtain the two-term inward recurrence formula

$$\hat{R}_n = U_n - \hat{R}_{n+1}^{-1} \tag{26}$$

This formula can be iterated down (i.e., for decreasing index n) once the value of the term $\hat{R}_N$ is specified. The grid point x_N is located at $x_N = x_f$ and from the discussion of boundary values in the previous section, the wavefunction has the values $\Psi(x_N) = 0$ and $\Psi(x_{N-1}) \neq 0$. The corresponding value of the inverse of $\hat{R}_N$ is $\hat{R}_N^{-1} = 0$.

In the Gordon procedure, the inward and outward solutions and their first deviatives were required to be equal at the matching point x_m [see Eqs. (9) and (10)]. An alternative requirement is that the inward and outward solutions are equal at the two adjacent grid points x_m and x_{m+1},

$$\Psi_l(x_m) \cdot 1 = \Psi_r(x_m) \cdot r = \psi(x_m) \tag{27}$$

and

$$\Psi_l(x_{m+1}) \cdot 1 = \Psi_r(x_{m+1}) \cdot r = \psi(x_{m+1}). \tag{28}$$

Multiply Eq. (27) by $(I - T_m)$ and Eq. (28) by $(I - T_{m+1})$ and use Eq. (18) to obtain

$$F_l(x_m) \cdot 1 = F_r(x_m) \cdot r = f(x_m) \tag{29}$$

and

$$F_l(x_{m+1}) \cdot 1 = F_r(x_{m+1}) \cdot r = f(x_{m+1}). \tag{30}$$

The vector quantity $f(x_n)$ is defined to be [this is the vector version of Eq. (18)]

$$f(x_n) = (I - T_n)\psi(x_n). \tag{31}$$

From the definitions of the ratio matrices, Eqs. (21) and (25), we can rewrite Eq. (30) in the form

$$R_m F_l(x_m) \cdot 1 = \hat{R}_{m+1}^{-1} F_r(x_m) \cdot r. \tag{32}$$

Then substitute from Eq. (29) to obtain

$$(R_m - \hat{R}_{m+1}^{-1})f(x_m) = 0. \tag{33}$$

Equation (33) will have a nontrivial solution only if

$$D(E) = |R_m - \hat{R}_{m+1}^{-1}| = 0. \tag{34}$$

Thus, the determinant $D(E)$, which is a function of the trial energy E, will vanish at each of the eigenvalues. The search for the zeros of $D(E)$ can be carried out by any standard one-dimensional search method. We have used the secant method[11] for this; it is easy to program and has a quite adequate convergence rate. As a precaution, the convergence of the secant method should be monitored, and if it starts to diverge, the program can return to the node count procedure to get closer to the eigenvalue before trying the secant method again. This method is only used as the final stage of convergency for nondegenerate eigenvalues. For degenerate eigenvalues the convergence is entirely by the node count procedure.

Not all points, x_m, which satisfy the relation $x_0 < x_m < x_N$ can serve as the matching point. The important problem of calculating an optimum value for x_m is discussed in Appendix C.

III. EIGENFUNCTION CALCULATIONS

In this section we present the renormalized Numerov method for computing the eigenfunctions and also a useful formula for interpolating the eigenfunctions between grid points.

It is assumed that an eigenvalue has already been calculated. With the energy parameter set equal to this eigenvalue, Eq. (22) is solved for the matrices R_1, R_2, ... R_m, and Eq. (26) is solved for $\hat{R}_{N-1}$, $\hat{R}_{N-2}$, ... $\hat{R}_{m+1}$. Since the determinant of the matrix $(R_m - \hat{R}_{m+1}^{-1})$ is zero, we can obtain a nontrivial solution of Eq. (33) for the column vector $f(x_m)$. If the eigenvalue is nondegenerate, the vector $f(x_m)$ is unique, to within an unimportant normalization factor. If the eigenvalue is g-fold degenerate then g linearly independent nontrivial solutions exist which can be constructed to be orthogonal to each other. The vectors $f(x_n)$ for $n < m$ are constructed by an iterative application of the formula

$$f(x_n) = R_n^{-1}f(x_{n+1}), \quad n = m - 1, \ m - 2, \cdots 0 \tag{35}$$

which is easily derived using Eq. (21) and the relation $f(x_n) = F_n \cdot 1$. Similarly the vectors $f(x_n)$ for $n > m$ are constructed by an iterative application of the formula

$$f(x_n) = \hat{R}_n^{-1}f(x_{n-1}), \quad n = m + 1, \ m + 2, \cdots N \tag{36}$$

which is obtained from Eq. (25) and the relation $f(x_n)$

$= \mathbf{F}_n \cdot \mathbf{r}$. The wavefunction $\psi(x_n)$ is then calculated at each grid point using Eq. (31).

For some problems it is convenient to know the value of the wavefunction at points other than the evenly spaced grid points. For these cases, it would be useful to have a simple formula for interpolating the wavefunction at an arbitrary point to the same accuracy as it is known at the grid points. Such a formula was derived for the one-dimensional problem[1] and it can easily be generalized to the multichannel problem. The derivation of the multichannel interpolation formula will not be presented here. It is identical to the derivation of the one-dimensional formula if we replace scalar quantities by their appropriate matrix generalizations. This multichannel interpolation formula is

$$\psi(x) = [(\alpha\beta)^{-1}\mathbf{I} + \gamma(x)]^{-1}\{[\beta^{-1}\mathbf{I} - \gamma(x_i)]\psi(x_i)$$
$$+[\alpha^{-1}\mathbf{I} - \gamma(x_{i-1})]\psi(x_{i-1})]\} \qquad (37)$$

where

$$x = x_{i-1} + \alpha h$$

$$h = x_i - x_{i-1}$$

$$\beta = (1 - \alpha), \quad 0 \le \alpha \le 1$$

and

$$\gamma(x) = -(h^2/6)\mathbf{Q}(x) \qquad (38)$$

The truncation error for this formula is of order h^4, which is the same as the cumulative error at a fixed value of x of the Numerov formula.[12]

IV. EXAMPLE CALCULATIONS AND DISCUSSION

A computer program based on the methods described in this paper has been written[13] and tested on a variety of problems. The results of several of these test problems are presented along with a general discussion in this section.

The first case is a nonisotropic three-dimensional harmonic oscillator. This system is separable and has an analytic solution in rectangular coordinates while in spherical coordinates it can be formulated as a coupled channel problem.

In rectangular coordinates the model Hamiltonian is

$$H = \tfrac{1}{2}[-\nabla^2 + x^2 + y^2 + \omega^2 z^2], \qquad (39)$$

where ω, the angular frequency in the z-direction, is a variable parameter. The highly degenerate set of eigenvalues of this system is given by

$$E = (n_x + n_y + 1) + \omega(n_z + \tfrac{1}{2}) \qquad (40)$$

where

$$n_i = 0, 1, 2, \ldots, \quad i = x, y, z.$$

In spherical coordinates the Schrödinger equation for this problem is

$$\left[-\frac{\partial^2}{\partial r^2} + \frac{L^2}{r^2} + r^2 + (\omega^2 - 1)r^2\cos^2(\theta) - 2E\right][r\psi(r, \theta, \varphi)] = 0, \qquad (41)$$

where L is the angular momentum operator

TABLE I. Exact and numerically calculated eigenvalues of the nonisotropic three-dimensional harmonic oscillator for $\omega = 1.5$.

n	k	Exact[a] $E_{n,k}$	Numerical[b] $E_{n,k}$
0	0	1.75	1.750000
1	0	3.75	3.750000
1	1	4.75	4.750000
2	0	5.75	5.749999
2	1	6.75	6.750000
2	2	7.75	7.749999
3	0	7.75	7.749999
3	1	8.75	8.750001
3	2	9.75	9.749999
4	0	9.75	9.750036

[a]Exact eigenvalues were calculated using Eq. (47).
[b]Numerical results were calculated in an eight-channel approximation.

$$[L^2 - l(l+1)]\,Y_{l,m}(\theta, \varphi) = 0 \qquad (42)$$

The wavefunction can be written as an expansion in spherical harmonics

$$r\psi^{(m)}(r, \theta, \varphi) = \sum_{l=|m|}^{\infty} f_l^{(m)}(r)\,Y_{l,m}(\theta, \varphi). \qquad (43)$$

Since the potential is cylindrically symmetric about the z-axis, the solutions can be constructed to be eigenstates of the z component of angular momentum and labeled with the quantum number m. In our example problem we will solve only for the $m = 0$ case and for convenience the superscript m will be omitted from now on. Substitute Eq. (43) into Eq. (41), use Eq. (42), multiply the resulting equation by $Y_{k,0}^*(\theta, \varphi)$ and integrate over the solid angle Ω to obtain the infinite set of coupled differential equations

$$\sum_{l=0}^{\infty}[(-d^2/dr^2 + l(l+1)/r^2 - 2E)\delta_{k,l} + (\omega^2 - 1)r^2 V_{k,l}]f_l(r) = 0, \qquad (44)$$

where

$$V_{k,l} = \int Y_{k,0}^*(\theta, \varphi)\cos^2(\theta)\,Y_{l,0}(\theta, \varphi)\,d\Omega. \qquad (45)$$

This integral is readily evaluated in terms of the Clebsch-Gordan coefficients[14]

$$V_{k,l} = \frac{2}{3}\left(\frac{2l+1}{2k+1}\right)^{1/2} C^2(l, 2, k; 0, 0, 0) + \tfrac{1}{3}\delta_{k,l}. \qquad (46)$$

Since $C(l, 2, k; 0, 0, 0) = 0$ unless $l + k + 2$ is even, the even integer subscripted terms (even parity) and the odd integer subscripted terms (odd parity) are decoupled from each other. We chose to solve for the even parity solutions.

The infinite sum over even terms in Eq. (44) was truncated to a finite sum and the resulting coupled channel Schrödinger equation was solved numerically for various assigned values of ω. Results for the case $\omega = 1.5$ are given in Table I where they are compared with

the exact analytic results. The analytic formula that applies to the $m = 0$, even parity case is

$$E_{n,k} = 2(n - k) + 1 + (2k + \tfrac{1}{2}) \omega, \tag{47}$$

where the quantum numbers n and k are

$$n = 0, 1, 2, \cdots \text{ and } 0 \le k \le n \tag{48}$$

A graphical representation of these eigenvalues is shown in Fig. 1.

Five distinct contributions to errors in the numerical results can be identified. Four of these, the truncation, tolerance, termination and roundoff errors are the same errors identified by Shore[15] in his discussion of the one-dimensional radial Schrödinger equation. The fifth contribution to the error was introduced when the infinite set of coupled differential equations, equivalent to the original multidimensional Schrödinger equation, was truncated to a finite set.

The results in Table I were calculated using an eight-channel approximation. It is interesting to note that the eigenvalues $E_{3,2}$ and $E_{4,0}$ which are degenerate in the exact calculation are not degenerate in the approximate calculation. This is an example of a spurious avoided crossing[16] in which two curves cross each other in an exact calculation but avoid each other in an approximate calculation. In order to show this more clearly we have computed $E_{3,2}(\omega)$ and $E_{4,0}(\omega)$ using only five coupled channels. The results are plotted in Fig. 2 where the avoided crossing behavior is clearly evident. The exact analytic results are also plotted for comparison. The relatively large error in this case is, of course, due to using only five channels. The $E_{2,2}$ and $E_{3,0}$ levels
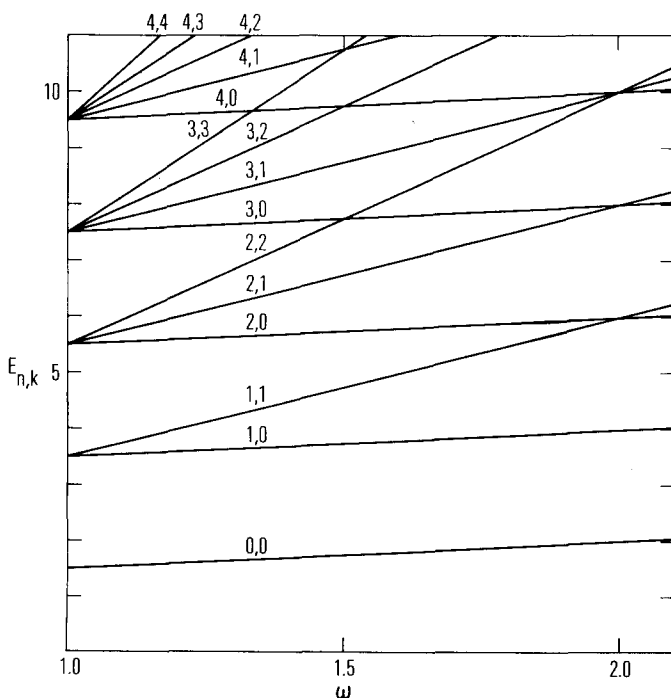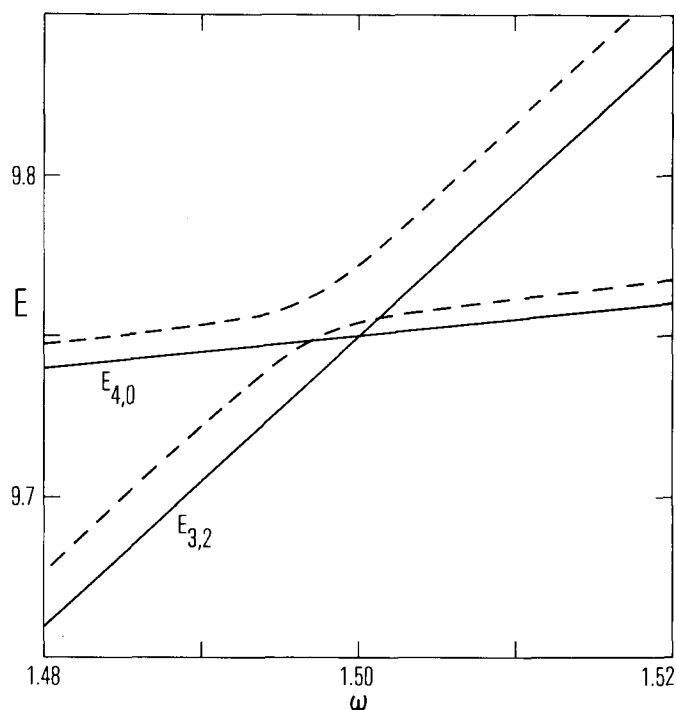
FIG. 2. Enlarged view of the $E_{3,2}$ and $E_{4,0}$ eigenvalues near the point of degeneracy. The solid curves are exact results, the dashed curves are the same eigenvalues calculated using a five-channel approximation. This is an example of a spurious avoided-crossing.[16]

also have avoided crossing in the multichannel approximation. However, in our eight-channel calculation, the separation of these levels at the avoided crossing is so small that they cannot be distinguished within the specified tolerance factor ϵ and so they were calculated to be degenerate.

The truncation error is a function of the grid spacing h. It is the result of replacing the differential equation, Eq. (5), with the approximate finite difference equation, Eq. (15). We have verified by numerical calculations that the truncation error is given by

$$\Delta E_{\text{trunc}} = C_4 h^4 + C_6 h^6 + \cdots \tag{49}$$

where C_4 and C_6 are unknown constants. This is consistent with the order h^4 accuracy of the Numerov method.[12] Equation (49) can be used to extrapolate the eigenvalues calculated for several different values of h to $h = 0$ by the Richardson method.[11] This is particularly useful if we require results with extremely small truncation errors. The results in Table I were calculated with a grid spacing $h = 0.03$.

The tolerance factor ϵ was mentioned previously in Sec. II. It is the accuracy that is requested of the calculation. When an eigenvalue has converged to within ϵ of its limiting value, the computation is terminated. In our example calculation, the tolerance factor was chosen to give convergence to approximately six or seven significant figures.

Roundoff error is inherent in most numerical calculations not utilizing integer arithmetic. It originates with

FIG. 1. Energy eigenvalues of the three-dimensional harmonic oscillator as a function of the parameter ω. These curves were calculated using Eq. (47), the labels are the quantum numbers n and k.

the finite number of digits used to represent the numbers on a digital computer and sets the ultimate bound on numerical accuracy. A discussion of this error is included in most texts on numerical analysis.[17] Our calculations were done on a CDC 7600 computer which represents numbers to about 14 decimal digits.

The termination error is introduced when we force the wavefunction to be zero at the artificial boundary point x_f (see the previous discussion of boundary conditions) instead of using the true boundary condition at infinity given by Eq. (3). In the present example problem $x_f = 6.0$.

Except for the roundoff error we can control the magnitudes of the error terms by an appropriate choice of parameters. Obviously, reducing any of these errors increases the computation time.

We have incorporated one other approximation into our program. It was mentioned previously that the determinental relation $|I - T_n| > 0$ is assumed to hold. If this relation is not true, it means that the grid spacing h is far too large for at least some components of the wavefunction. One result will be an incorrectly computed node count. A solution to this problem is to decrease h, however, this increases the computing time and is usually not necessary. The difficulty usually occurs near the origin where the diagonal elements of the potential matrix can become extremely large and positive in value. The simplest solution to this problem begins by recognizing that the components of the wavefunction affected by the large potential elements are negligibly small in this region. They are so small, in fact, that the potentials can be truncated to some high value without affecting the solution in any significant way. Therefore, we designed our program to automatically truncate all diagonal potential elements so that the relation $|I - T_n| > 0$ always holds.

The second test case considered is the single-center expansion of the hydrogen molecular ion. This is an important problem that has been discussed by several authors.[18–20] Our purpose is not to add significantly to this discussion but to simply use this problem as a convenient test case for our numerical procedure.

The two hydrogen nuclei A and B are clamped to the z-axis. Nucleus A is located at R and B is located at $-R$. The Hamiltonian is (in atomic units)

$$H = -\tfrac{1}{2}\nabla^2 - 1/r_A - 1/r_B, \tag{50}$$

where r_A and r_B are the distances of the electron from A and B. The potential can be expanded in Legendre polynomials

$$r_A^{-1} + r_B^{-1} = 2\sum_n (r_<^{2n}/r_>^{2n+1})\, P_{2n}(\cos\theta), \tag{51}$$

where $r_< = \min(r, R)$ and $r_> = \max(r, R)$. The procedure for formulating this problem as an infinite set of coupled differential equations is the same as in the previous case. The result is

$$\sum_{l=0}^{\infty}\left[(-d^2/dr^2 + l(l+1)/r^2 - 2E)\,\delta_{k,l} + V_{k,l}(r)\right]f_l(r) = 0, \tag{52}$$

TABLE II. Single center expansion calculated energies of the $1s\sigma_g$ and $2s\sigma_g$ states of H_2^+ as a function of the number of expansion terms. The internuclear separation is 2 bohr. Energies are in atomic units.

N	$1s\sigma_g$	$2s\sigma_g$
2	-1.08368	-0.35845
4	-1.09997	-0.36051
6	-1.10184	-0.36076
8	-1.10230	-0.36082
10	-1.10246	-0.36084
exact[25]	-1.10263	-0.36086

where

$$V_{k,l}(r) = -4\sum_{n=0}^{\infty} (r_<^{2n}/r_>^{2n+1}) \int Y_{k,m}^*(\theta,\varphi)$$
$$\times P_{2n}(\cos\theta)\, Y_{l,m}(\theta,\varphi)\,d\Omega. \tag{53}$$

The integral in Eq. (53) is most conveniently evaluated in terms of Clebsch–Gordan coefficients.[14] Restricting our attention to the case $m=0$, we obtain

$$V_{k,l}(r) = -4\left(\frac{2l+1}{2k+1}\right)^{1/2} \sum_{n=|l-k|}^{l+k}$$
$$\times (r_<^{2n}/r_>^{2n+1})\, C^2(l, 2n, k; 0, 0, 0). \tag{54}$$

We also restrict our test calculations to the even parity solutions.

We solved for the $1s\sigma_g$ and $2s\sigma_g$ states with $R=1$ bohr. The results of these calculations are given in Table II. The $1s\sigma_g$ results can be compared to the results obtained by Ali and Meath.[20] They solved the coupled differential equations by the method of Fox.[2] The four-channel result also is in excellent agreement with the extrapolated four-term result of Cohen and Coulson.[18]

The cusp in the potential matrix elements at $r = R$ [see Eq. (54)] adversely effects the truncation error. We have established numerically that the truncation error for this problem is given by[21]

$$\Delta E_{\text{trunc}} = C_2 h^2 + C_4 h^4 + \cdots \tag{55}$$

This is a much slower convergence rate than in the previous case [see Eq. (49)]. Because of this slow rate, we used the Richardson extrapolation method to calculate the results in Table II. The two-grid spacings used in this extrapolation were $h = 0.04$ and $h = 0.02$.

Since the full inherent accuracy of the Numerov method is not being utilized in this problem, we could have saved computer time by using a simpler finite difference approximation than Eq. (15), i.e., one that has a cumulative truncation error of only $O(h^2)$. A simple formula that meets this requirement is

$$\Psi_{n+1} - U_n\Psi_n + \Psi_{n-1} = 0, \tag{56}$$

where

$$U_n = 2I - h^2 Q_n. \tag{57}$$

These equations replace Eqs. (19) and (20) respectively.

The wavefunction matrix Ψ_n replaces F_n in Eq. (19) and in all subsequent equations. Since no inversion is required to evaluate Eq. (57), one of the two matrix inversions per grid point has been eliminated. In most problems, the increased computation time of the Numerov formula is more than offset by its decreased truncation error. However, this is not the case for the present problem where we have verified that the truncation error is about the same for both methods.

The third test case is a two-channel problem designed to demonstrate the stability of our method against large potential barriers. Define the Gaussian function

$$G(x) = 5000 \exp[-200(x - 1.6)^2] \tag{58}$$

and the Morse function

$$M(x) = 31\,250 \left| 1 - \exp[- B(x - 1.5)] \right|^2. \tag{59}$$

where $B = 1.540375616035$. Let the reduced mass for this problem be $\mu = (2B^2)/(8\hbar^2)$. The potential matrix elements are defined to be

$$V_{11}(x) = V_{22}(x) = M(x) + G(x) \tag{60}$$

and

$$V_{12}(x) = V_{21}(x) = G(x) \tag{61}$$

This potential matrix can be diagonalized by a constant orthogonal matrix. The resulting two uncoupled potentials are the Morse potential and the unsymmetric double minimum potential used in Ref. (1). In the present test we did not do this diagonalization, but rather solved it as a coupled channel problem. The eigenvalues calculated were the same as the merged (and rearranged in order of increasing value) results given in Tables I and II in Ref. 1.

The eigenfunctions of a system that is symmetric about the point x_s are symmetric and antisymmetric about x_s. Just as in the one-dimensional case,[1] we can take advantage of this to reduce the computation time by integrating over only half the range, $x \geq x_s$. The antisymmetric solutions are calculated by merely letting x_s be the initial boundary point of the integration range. Since the antisymmetric functions are zero at x_s, the initial boundary values are the same as we have been using, i.e., $R_0^{-1} = 0$, so no changes are required in the program. The symmetric functions, on the other hand, have zero slope at x_s. Let Ψ_{-1}, Ψ_0, and Ψ_1 be the values of the wavefunction matrix at the grid points $x_{-1} = x_s - h$, $x_0 = x_s$, and $x_1 = x_s + h$. From symmetry it follows that $\Psi_{-1} = \Psi_1$ and therefore from Eqs. (17) and (18) we obtain $F_{-1} = F_1$. Substituting this into Eq. (19) and using Eq. (21) we obtain the initial value of the ratio matrix, $R_0 = 0.5U_0$ where U_0 is defined by Eq. (20).

APPENDIX A

In this appendix several peripherally related topics are discussed. These include: a generalization of the log derivative method to the multichannel bound state problem; a derivation of the formulas for computing the log derivative matrix from the ratio matrix computed by the renormalized Numerov method; and finally, a comment on the calculation of the scattering matrix by a renormalized Numerov calculation.

The log derivative matrix is defined to be[22]

$$y(x) = \Psi'(x)\Psi^{-1}(x), \tag{A1}$$

where $\Psi(x)$ is the solution of Eq. (5). It satisfies the matrix Ricatti equation

$$y'(x) + Q(x) + y^2(x) = 0. \tag{A2}$$

A numerical method of solving this equation is discussed in Ref. (22). In Sec. II of this paper we defined a multichannel node to be a zero of the function $|\Psi(x)|$. From Eq. (A1), it is evident that this corresponds to a pole of the determinant of the log derivative matrix, $|y(x)|$. These poles can be counted by monitoring the numerical solution at each grid point and counting the number of times the relation $h|y(x_n)| < -1$ is encountered. The explanation of this is similar to that given in Ref. (1) for the one-dimensional case. Utilizing this technique we can implement the node count procedure for locating eigenvalues described in this paper.

The fast converging method of locating eigenvalues by inward and outward integration to a common matching point x_m can also be implemented. The multichannel matching conditions are given by Eqs. (9) and (10). From the definition of the log derivative matrix, Eq. (A1), it is obvious that we can rewrite Eq. (10) in the form

$$y_l(x_m) \Psi_l(x_m) \cdot 1 = y_r(x_m) \Psi_r(x_m) \cdot r. \tag{A3}$$

Then substituting from Eq. (9) we obtain

$$[y_r(x_m) - y_l(x_m)]\psi(x_m) = 0. \tag{A4}$$

Nontrivial solutions to this equation will only exist at the energies for which the relation

$$|y_r(x_m) - y_l(x_m)| = 0 \tag{A5}$$

is satisfied. Energies which satisfy this matching condition are located by a one-dimensional search method. At these energies Eq. (A4) can then be solved for $\psi(x_m)$.

The matching condition, Eq. (A5), can also be derived directly from the Gordon form of the matching condition given by Eq. (12). Evaluating the determinant in Eq. (12) in terms of the submatrices, we obtain

$$d(E) = |\Psi_l(x_m)| \cdot |\Psi_r'(x_m) - \Psi_l'(x_m) \Psi_l^{-1}(x_m) \Psi_r(x_m)| = 0. \tag{A6}$$

A condition on the location of the matching point x_m is that it must not coincide with a node of either the incoming or outgoing wavefunction (this is discussed further in Appendix B), i.e., $|\Psi_l(x_m)| \neq 0$ and $|\Psi_r(x_m)| \neq 0$. From this and Eq. (A6) it follows that

$$|\Psi_r'(x_m) \Psi_r^{-1}(x_m) - \Psi_l'(x_m) \Psi_l^{-1}(x_m)| = 0. \tag{A7}$$

Using the definition of the log derivative, Eq. (A1), we again obtain the matching condition, Eq. (A5).

In Ref. 1 we derived formulas for computing the log derivative of the wavefunction by a renormalized Numerov calculation. Here we give the multichannel generalization. Using Eqs. (18) and (21) we obtain

$$\Psi_{n+1} = [I - T_{n+1}]^{-1} R_n F_n \tag{A8}$$

$$\Psi_n = [I - T_n]^{-1} F_n \tag{A9}$$

$$\Psi_{n-1} = [I - T_{n-1}]^{-1} R_{n-1}^{-1} F_n \tag{A10}$$

The matrix version of Blatts formula[8] for the derivative of the wavefunction is

$$\Psi'_n = h^{-1}[(0.5I - T_{n+1})\Psi_{n+1} - (0.5I - T_{n-1})\Psi_{n-1}].$$ (A11)

Substitute Eqs. (A8) and (A10) into this formula, then multiply this expression on the right by the inverse of Eq. (A9) to obtain

$$y(x_n) = h^{-1}(A_{n+1}R_n - A_{n-1}R_{n-1}^{-1})(I - T_n),$$ (A12)

where

$$A_n = (0.5I - T_n)(I - T_n)^{-1}.$$ (A13)

By a similar analysis, we can also derive a formula utilizing the inward integrated ratio matrices defined by Eq. (25). We obtain

$$y(x_n) = h^{-1}(A_{n+1}\hat{R}_{n+1}^{-1} - A_{n-1}\hat{R}_n)(I - T_n).$$ (A14)

Although this paper is primarily devoted to the application of the renormalized Numerov method for calculating bound state solutions, it seems appropriate to briefly point out how it can also be used to calculate the S-matrix for a scattering problem.

We have two methods to accomplish this. The first procedure is to calculate the log derivative matrix using Eq. (A12) and then calculate the S-matrix using the formulas given in Ref. (22).

The second procedure avoids the intermediate step of calculating the log derivative matrix. In the asymptotic region, $x \geq x_N$, where all but the centrifugal term of the potential has become negligible, the wavefunction is

$$\Psi(x) \underset{x \geq x_N}{=} J(x) + N(x)K$$ (A15)

The notation used here is the same as in Ref. (22), K is the (augmented) reaction matrix and $J(x)$ and $N(x)$ are diagonal matrix functions. The diagonal elements of $J(x)$ and $N(x)$ are the Riccati–Bessel function solutions of Eq. (5) obtained when only the centrifugal potential term is acting. For convenience define a new set of diagonal matrix functions (defined only at the grid points)

$$j(x_n) = (I - T_n)J(x_n)$$ (A16)

and

$$n(x_n) = (I - T_n)N(x_n),$$ (A17)

where T_n, defined by Eqs. (17) and (2), is evaluated using only the centrifugal potential. Multiplying Eq. (A15) by $(I - T_n)$ we obtain

$$F_n \underset{x_n \geq x_N}{=} j(x_n) + n(x_n)K,$$ (A18)

where Eqs. (18), (A16), and (A17) have been used. Evaluate Eq. (A18) at x_N and x_{N+1}, calculate the ratio matrix $R_N = F_{N+1}F_N^{-1}$, then solve the resulting equation for K in terms of R_N

$$K = -[R_N n(x_N) - n(x_{N+1})]^{-1}[R_N j(x_N) - j(x_{N+1})].$$ (A19)

The S-matrix is then calculated from the K-matrix by the formulas given in Ref. 22.

The closed channel elements of $J(x)$ increase exponentially while for $N(x)$ they decrease exponentially

with increasing x. This can be a source of numerical difficulty in evaluating Eq. (A19). The problem is easily eliminated by a procedure similar to that used in Ref. (22). Replace the closed channel elements of $j(x_N)$, $j(x_{N+1})$, $n(x_N)$ and $n(x_{N+1})$ by

$$[j(x_{N+1})]_{ii} \rightarrow [j(x_{N+1})]_{ii}[j(x_N)]_{ii}^{-1}$$ (A20)

$$[j(x_N)]_{ii} \rightarrow 1$$ (A21)

$$[n(x_{N+1})]_{ii} \rightarrow [n(x_{N+1})]_{ii}[n(x_N)]_{ii}^{-1}$$ (A22)

and

$$[n(x_N)]_{ii} \rightarrow 1$$ (A23)

It is easily verified that this transformation will leave the elements of the K-matrix which connect open channels to open channels unchanged. Therefore, the S-matrix is also unchanged.

APPENDIX B

In this appendix we discuss the method of counting nodes when more than one node is located between two adjacent grid points. The nature of this problem is most easily seen by considering an uncoupled multichannel problem. The wavefunction matrix $\Psi(x)$ and the ratio matrix R_n are both diagonal in this case. If two of the diagonal elements of $\Psi(x)$ have nodes between x_n and x_{n+1} the determinantal function $|\Psi(x)|$, which is the product of the diagonal elements, will not change sign and therefore $|R_n|$ will not be negative. Thus, we have missed counting two nodes. Obviously any odd number of nodes will be counted only once and any even number will not be counted at all. Such a situation can also occur when the channels are coupled. The problem is easily resolved in the uncoupled case; we simply monitor all the diagonal elements of the matrix R_n and increase the count by one every time one of them is less than zero. We have devised an efficient method that reduces to this in the decoupled limit. We have not been able to prove that this method must work when the channels are coupled, however, it has worked on all the test problems that have been tried so far. In any case, even if this method were to fail, we are in no danger of computing a wrong answer since a wrong node count in one of the stages of iteration would cause an inconsistency that would be detected and stop the calculation. The determinant of R_n is computed in the same Gaussian elimination calculation as the inverse of R_n. Although L and U are not explicitly computed, Gaussian elimination is equivalent to making a triangular decomposition[23] of R_n, i.e., $R_n = LU$. Here L is a lower triangular matrix with ones on the diagonal. The determinant is the product of the diagonal elements of the upper triangular matrix U. Our method of counting nodes is equivalent to monitoring each of the diagonal elements of U and to increasing the node count by one each time one of them is negative.

APPENDIX C

In this appendix we discuss the method used to calculate the position of the matching point x_m. Assume that suitable upper and lower energy bounds, E_H and E_L with a single eigenvalue between them, has been
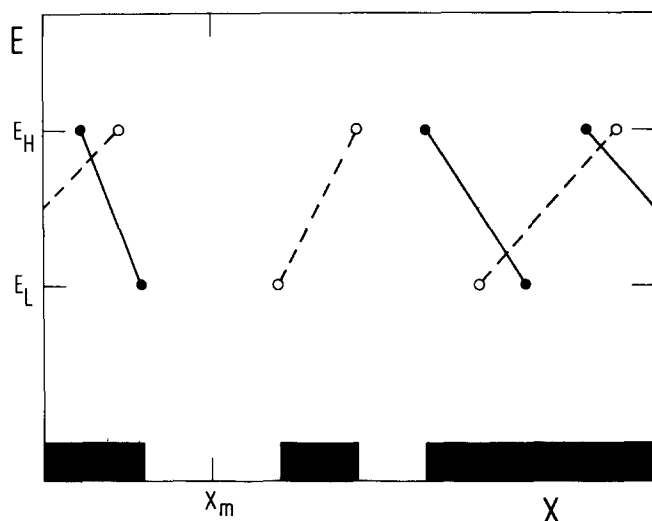
FIG. 3. Schematic of nodes and node trajectories in the E, x plane. The solid lines are the trajectories for nodes calculated by outward integration, the dashed lines are trajectories calculated by inward integration. The blocks cover the regions of x traversed by nodes in the energy interval E_L to E_H. The matching point x_m is centered in the largest node free region.

established by the node count procedure. Then solve the outward recurrence relation, Eq. (22), and locate all the nodes at the two energies E_L and E_H. These are represented schematically in Fig. 3 by the solid dots. The nodes trace continuous trajectories in the two-dimensional (E, x) space. As E is increased the nodes move monotonically to the left. When the parameter E is just equal to the energy eigenvalue between E_L and E_H a new node is created at the right boundary. All this is represented schematically in Fig. 3 by the solid lines connecting the nodes. Similarly, we can solve the inward recurrence relation, Eq. (26), and locate the nodes[24] of the inward solutions for the energies E_L and E_H. These are represented by the open dots in Fig. 3. In the intervening energy interval, these nodes move monotonically to the right as the energy is increased. The trajectories are represented by the dashed lines.

The only requirement on the matching point x_m is that it should not be near a node of either the inward or outward solutions in the E_L to E_H energy range. The blocks in Fig. 3 cover those regions of x traversed by both the inward or outward sets of nodes. The remaining regions, not covered by blocks, are node free. The program searches for the largest of these node free regions and locates x_m at its center.

APPENDIX D

In most cases, the initial value of the inverse of the ratio matrix is $R_0^{-1} = 0$. All the example problems presented in Sec. IV follow this rule. Exceptional cases do occur, however. A notable example of this is the calculation of the bound states of the hydrogen atom. In this appendix we will give a general method for calculating R_0 and then apply it to the hydrogen atom problem as an example case.

The method is quite simple. Combining Eqs. (5),

(17) and (18) we obtain the result

$$\mathbf{F}_n = \mathbf{\Psi}(x_n) - (\hbar^2/12) \mathbf{\Psi}''(x_n), \tag{D1}$$

where the double prime means the second derivative with respect to x. Since the wavefunction is zero at $x_0 = 0$, we obtain

$$\mathbf{F}_0 = -(\hbar^2/12) \mathbf{\Psi}''(0) \tag{D2}$$

and at $x_1 = h$

$$\mathbf{F}_1 = \mathbf{\Psi}(h) - (\hbar^2/12) \mathbf{\Psi}''(h). \tag{D3}$$

These expressions are easily evaluated by computing a power series expansion of the wavefunction about the origin. Terms through the cubic should be retained in order to be compatible in accuracy with the Numerov method. Then use Eq. (21) to calculate R_0.

From this analysis we see that the exceptional cases which do not obey the rule $R_0^{-1} = 0$ are those in which the second derivative of the wavefunction is nonzero at the origin.

As an example of using this method, it will be applied to the hydrogen atom problem. The Schrödinger equation (in atomic units) is

$$\left[\frac{d^2}{dx^2} + \frac{2}{x} - \frac{l(l+1)}{x^2} + 2E \right] \psi(x) = 0. \tag{D4}$$

Expand the wavefunction in a power series

$$\psi(x) = x^n (1 + bx + cx^2 + \cdots) \tag{D5}$$

Substitute this into Eq. (D4) and evaluate the parameters n, b, and c. The result is

$$n = l + 1 \tag{D6}$$

$$b = -(l+1)^{-1} \tag{D7}$$

and

$$c = -(2l+3)^{-1}[(l+1)^{-1} - E] . \tag{D8}$$

Substitute these into Eq. (D5), then evaluate F_0 and F_1 and calculate R_0. The following results are obtained:

$$R_0 = 6/h - 5 + (1 - E)h; \quad l = 0 \tag{D9}$$

$$R_0 = -5 + (3/2)h; \quad l = 1 \tag{D10}$$

and

$$R_0 = \infty; \quad l \geq 2. \tag{D11}$$

Thus, it is only the $l = 0$ and $l = 1$ cases that require any change from our rule, $R_0^{-1} = 0$. Since R_0 is negative in the $l = 1$ case, care must be taken so that we do not count an extra wavefunction node.

We have verified this procedure by numerically computing the bound states of hydrogen. The error in the computed eigenvalues was greatly reduced when correct values of R_0 were used in the $l = 0$ and $l = 1$ cases compared to the results obtained using $R_0^{-1} = 0$.

[1]B. R. Johnson, J. Chem. Phys. 67, 4086 (1977).
[2]See the appendix by L. Fox in Ref. (18).
[3]L. Fox, Boundary-value Problems in Differential Equations, (edited by R. E. Langer, University of Wisconsin Press, Madison, 1960), pp. 243–56.

[4]R. G. Gordon, J. Chem. Phys. **51**, 14 (1969).

[5]A. M. Dunker and R. G. Gordon, J. Chem. Phys. **64**, 4984 (1976).

[6]L. D. Landau and E. M. Lifshitz, *Quantum Mechanics*, (Pergamon, New York, 1965).

[7]B. R. Johnson, Chem. Phys. **2**, 381 (1973).

[8]J. M. Blatt, J. Comp. Phys. **1**, 382 (1967).

[9]In a recent publication M. LeDourneuf and Vo Ky Lan, J. Phys. B **10**, L35 (1977), implied that numerical methods which invert matrices at each step are inefficient compared to those which multiply matrices at each step. Actually, the inversion of a symmetric matrix by Gaussian elimination requires fewer operations (and by actual test calculations uses less computer time) than the multiplication of two matrices of the same dimensions.

[10]In the limit $h \to 0$, it is obvious from Eq. (17) that $|\mathrm{I}\text{-}T_n| \to 1$. If this determinant deviates too far from its limiting value, it means that the grid spacing h is too large, producing a large truncation error. In the extreme case in which $|\mathrm{I}\text{-}T_n| < 0$, the numerical solution will break into an unphysical oscillation with a node at every grid point. This problem is discussed further in Sec. IV.

[11]A. Ralston, *A First Course in Numerical Analysis*, (McGraw-Hill, New York, 1965).

[12]I. H. Sloan, J. Comp. Phys. **2**, 414 (1968).

[13]The program as written will compute degenerate and non-degenerate eigenvalues and also the eigenfunctions of non-degenerate eigenvalues. At the present, it will not compute the eigenfunctions of degenerate eigenvalues.

[14]M. E. Rose, *Elementary Theory of Angular Momentum*, (Wiley, New York, 1957).

[15]B. W. Shore, J. Chem. Phys. **59**, 6450 (1973).

[16]G. J. Hatton, Phys. Rev. A **14**, 901 (1976); G. J. Hatton, W. L. Lichten, and N. Ostrove, J. Chem. Phys. **67**, 2169 (1977); G. J. Hatton, W. L. Lichten, and N. Ostrove, Chem. Phys. Lett. **40**, 437 (1976); C. M. Meerman-van Benthem, A. H. Huizer, and J. J. C. Mulder, Chem. Phys. Lett. **51**, 93 (1977).

[17]See for example, P. Henrici, *Elements of Numerical Analysis* (Wiley, New York, 1964), Chap. 16.

[18]M. Cohen and C. A. Coulson, Proc. Cambridge Philos. Soc. **57**, 96 (1961).

[19]M. Cohen, Proc. Cambridge Philos. Soc. **58**, 130 (1961).

[20]M. K. Ali and W. J. Meath, Int. J. Quant. Chem. **12**, 35 (1977).

[21]The truncation error for the H_2^+ problem is given by Eq. (55) only if one of the grid points, in each calculation at a different value of h, is located at the cusp of the potential.

[22]B. R. Johnson, J. Comp. Phys. **13**, 445 (1973).

[23]W. G. Strang and G. J. Fix, *An Analysis of the Finite Element Method*, (Prentice-Hall, Englewood Cliffs, 1973), pp. 34–35.

[24]The nodes of the inward solution are counted by counting the number of times the relation $|\hat{R}_n| < 0$ occurs. Multiple nodes between two grid points are handled as explained in Appendix B.

[25]M. Madsen and J. Peck, At. Data **2**, 171 (1971).